

ASITP

INSTITUTE OF THEORETICAL PHYSICS

ACADEMIA SINICA

AS-ITP-92-83

Dec. 1992

AN UPPER LIMIT FOR THE ELECTRON  
ANTI-NEUTRINO MASS FROM  
TRITIUM  $\beta$  DECAY

Dongqi LIANG

Shiping CHEN

et. al

FERMILAB  
LIBRARY  
MAR 01 1992

P.O.Box 2735, Beijing 100080, The People's Republic of China

Telefax : (086)-1-2562587

Telephone : 2568348

Telex : 22040 BAOAS CN

Cable : 6158

AS-ITP-92-83



**An upper limit for the electron anti-neutrino mass from  
tritium  $\beta$  decay**

Liang Dongqi, Chen Shiping, Si Guojian, Chen Zhicai, Mao Yajun

Hu Zhonglin, Mao Naifeng, Sun Qinren, Du Hongshan, Li Zhimin

Liang Shengzhu, Wang Bidan, Wang fucheng, Yang Qing and Sun Hancheng

*( China Institute of Atomic Energy*

*P. O. Box 275(10), Beijing 102413 )*

Mei Zhenyue

*( University of Science and Technology of China, Hefei 230046 )*

Ching Chengrui

*( Center of Theoretic Physics, CCAST (World Laboratory) and*

*Institute of Theoretical Physics, Academia Sinica*

*P.O. Box 2735, Beijing 100080 )*

**ABSTRACT** - The end point region of the tritium  $\beta$ -spectrum is measured using a double focusing magnetic spectrometer. For the electron anti-neutrino mass an upper limit of  $m_{\bar{\nu}_e} < 12.1$  eV at 95% C.L. is obtained.

\*Supported by the National Natural Science Foundation of China

## 1 INTRODUCTION

For more than fifty years physicists have paid considerable attention to whether a neutrino has rest mass or not, an important problem in the fields of particle physics and astro-physics. Because of the difficulties in experiments, only the upper limits of the neutrino mass were reported.

In 1980, the ITEP group[1] published the evidence for non-zero  $m_{\nu}$ . In their later work, they proceeded improve their experimental instruments and methods, and came to the same conclusion — the electron anti-neutrino has finite mass, and a value of  $17 \text{ eV} < m_{\bar{\nu}_e} < 40 \text{ eV}$  was reported in their latest paper[2]. The same experiment has been repeated using different magnetic spectrometers in different laboratories [3-7], none of them has got a result, indicating a finite neutrino mass.

Since 1981, the neutrino mass experiment has been in its development in CIAE. A new iron-core  $255^\circ$  double focusing magnetic separator was reconstructed as a high resolution  $\beta$  spectrometer with high luminosity for our measurement. The preliminary result of our measurement was reported in 1986 at Osaka symposium[8]. Since then, some calibration experiments have been performed and the experimental data have been re-processed. This paper is the final report of our measurement.

## 2 THE MEASURING INSTALLATION

The central trajectory radius of the CIAE double focusing  $\beta$  spectrometer is  $r_0=40$  cm, the gap height 25 cm and the corresponding focusing angle is  $\theta_f=255^\circ$ . The initial

horizontal and vertical angles of the electron beam are within the ranges of  $\pm 9^\circ$  and  $\pm 1.5^\circ$ , respectively and are defined by five apertures at different places, with a corresponding transmission coefficient of 0.13% and a momentum resolution of 0.02% in theory for monoenergetic linelike electron source[9].

For raising the luminosity of the spectrometer, we used Bergkvist[10] method of an extended source of  $10 \times 9 \text{ cm}^2$  with both energy and geometry compensation on the basis of electron optics. It was shown that the electrostatic potential distribution on the source surface and the geometry of the source should meet some requirements. As shown in Fig. 1, the incline angle between the source surface and the  $\theta=0^\circ$  plane at  $r=r_0$  is  $48^\circ$ . The electrostatic potential with special distribution is applied on the source surface. To meet the above mentioned requirements, in theoretic calculation, we divided the  $\beta$  source into a series of narrow strips each 0.05 cm in width. These strips were curved in the radius of curvature of about 16 cm, concaved to the centre of the spectrometer, so as to obtain a straight image on the detector. Under these conditions, the theoretical momentum resolution of the spectrometer was about 0.1% and the luminosity was  $0.12 \text{ cm}^2$  [11].

The instability of the current to drive the magnet is less than  $10^{-4}$  in a two-day's run. A point-like electron gun of 18.6 keV was used for calibration[12]. In the case of optimum resolution condition the momentum resolution was 0.02%, which is in agreement with the theoretical calculation. Seventeen monoenergetic lines from  $^{170}\text{Tm}$ ,  $^{169}\text{Yb}$  and  $^{182}\text{Ta}$  were measured so that the linearity of the spectrometer could be tested.

A tritium labelled [3, 4, 5, 6-3H]PAD ( $\text{C}_{14}\text{H}_{15}\text{T}_3\text{O}_2\text{N}_3$ ) of high specific activity was prepared. This tritium source is  $\sim 2 \mu\text{g}/\text{cm}^2$  thick which was measured by backscattering method[13] and  $9.0 \times 3.0 \text{ cm}^2$  in effective dimensions with the total strength of the source is about 70 mCi. The source backing is a high resistive film of  $10^7 \Omega$ , through which the compensation potential is applied.

In order to measure the resolution function accurately, reference sources of monoenergetic internal conversion lines of  $^{169}\text{Yb}$  and  $^{170}\text{Tm}$  were used. The sources were vacuum evaporated on a pure aluminium backing and were cut into arc-like strips each 0.05 cm in width and 16 cm in radius of curvature. The source thickness is about  $2 \mu\text{g}/\text{cm}^2$ , and the radioactivity is about  $100 \mu\text{Ci}/\text{cm}^2$ , while the non-uniformity is less than 10% [14]. The strips of Yb and Tm sources were uniformly distributed on the high resistive backing which was similar to the backing of the tritium source.

The detector[15] is a thin window proportional counter with P10 gas as working gas at a pressure of  $3.3 \times 10^4 \text{ Pa}$ . The window is made of two or three layers of Formvar foils each in the thickness of  $100 \mu\text{g}/\text{cm}^2$ . For the 23 keV electrons, the energy loss in the window is less than 2 keV, and the transmission factor is more than 95%. The data acquisition was performed by using a system composed of a low-noise charge-sensitive preamplifier, a linear amplifier and a multichannel analyzer. The energy resolution for the photo-peak of 5.9 keV X-rays of  $^{55}\text{Fe}$  is 18%.

### 3 MEASURING METHOD AND RESOLUTION FUNCTION

Electrostatic scanning with constant magnetic field was used for measurement

of spectra, so that the hysteresis effect of the iron core of the spectrometer and the correction of the detector efficiency were avoided. However, the accepting solid angle of the spectrometer is a function of the scanning potential and was corrected experimentally by using  $^{169}\text{Yb-M}$  and  $^{170}\text{Tm-K}$  conversion lines with different scanning potentials[16].

The electrons emitted from the central line of the extended source were accelerated to 22.9 keV such that the pulse height of the tritium  $\beta$  spectrum in the end point region is larger than most of the background. In the most sensitive region for  $m_\nu$  (in 100 eV range below the end point energy of the tritium  $\beta$  spectrum), the signal to background ratio is approximately 1:1.

Generally, neutrino mass is calculated according to the spectral shape around the end of the tritium  $\beta$  decay spectrum obtained by a magnetic spectrometer. But a  $\beta$  spectrometer itself has electron optical resolution function and the  $\beta$  source suffers energy loss and backscattering, they both may make the  $\beta$  energy spectrum distorted, and hence, have a serious influence in the neutrino mass estimation. It is this account that a careful analysis was carried out theoretically and experimentally on the total resolution function[17].

The procedure for acquiring the total resolution function theoretically is shown in Eq. (1)

$$R_h = R_l \oplus (\Gamma \oplus EL \oplus SUO) \oplus ELS \quad (1)$$

where,  $R_l$  is the internal conversion spectrum for 18.437 keV electrons of  $^{169}\text{Yb-M1}$  line obtained under the same geometrical condition for the tritium  $\beta$  source. The measured spectra for Yb-M1, M2 and M3 lines as shown in Fig. 2;  $\Gamma$ , EL and ELS are the natural width of  $^{169}\text{Yb-M1}$  line and the energy loss spectra for monoenergetic electrons in Yb source and for the tritium  $\beta$  source, respectively, calculated by Monte Carlo simulation [18]; SUO is the spectrum of the shake up/off effect of Yb source[19].  $\ominus$  and  $\oplus$  stand for the calculation procedures of deconvolution and convolution.

Equation (2) gives the procedure for obtaining the total resolution function by experimentation.

$$R_{exp} = R_l \ominus R_s \oplus R_{ph} \oplus ELS \quad (2)$$

Here  $R_l \ominus R_s$  stands for the deconvoluting narrow strip ( $0.05 \times 3.0 \text{cm}^2$ ) from the large area ( $9 \times 8 \text{cm}^2$ ) internal conversion electron spectrum of  $^{169}\text{Yb}$  and  $^{170}\text{Tm}$  obtained experimentally;  $R_{ph}$  is the narrow photoelectron spectrum. The electron spectra of  $R_l$  and  $R_s$  are supposed to have the same  $\Gamma$ , SUO and EL in Eq. (2). The total resolution functions from  $^{169}\text{Yb-M1}$  and  $^{170}\text{Tm-K}$  internal conversion electron spectra, as based on Eq.(1) and (2), are shown in Fig 3, respectively.

Comparing the above mentioned total resolution functions from the two methods, we see that the FWHM of the total resolution functions is  $30 \pm 2 \text{eV}$  and the spectra are well comparable at the high energy side. At the low energy side the tail is higher for the theoretically calculated spectrum.

Obviously, the experimental method can avoid a lot of errors and uncertainties from theoretical calculation. This is just the distinction of the experimental method in which we acquired the total resolution functions. While neutrino mass is calculated by fitting  $m_\nu^2$ , the difference between the values of  $m_\nu^2$  from  $R_{th}$  and  $R_{exp}$  is accounted into the systematic error at the next section.

#### 4 DATA ACQUISITION AND ANALYSIS

The tritium  $\beta$  spectra were measured in the energy ranges of 17.4 – 23 keV or 17.8 – 23 keV. Fig. 4 is a typical  $^3\text{H}$ - $J$  pulse height spectrum of the proportional counter for the energy point of 17.35 keV. The small peak on the right hand side is the pulse height spectrum of  $^3\text{H}$ - $J$  rays. The high peak on the left is the pulse height spectrum of  $^{55}\text{Fe}$ -X (5.395 keV) source monitoring the stability of the counting system. The tritium spectrum is about 70 data points for each run which spent about 20 hrs., and the total acquisition time is about 2500 hrs.

The neutrino mass was estimated by least squares fitting of the following theoretical expression of  $N_{th}(E)$  to the measured spectrum:

$$N_{th}(E) = A\epsilon(E) \sum_i \{ F(Z, E_i) p E_i [1 + \alpha(E_0 - E_i)^2] \sum_j W_j n(E_i, E_j) \} \times R(E, E_i) + BG \quad (3)$$

$$n(E_i, E_j) = (E_0 - E_i - E_j) [(E_0 - E_i - E_j)^2 - m_\nu^2]^{1/2}$$

where,  $A$  is the normalization constant;  $F(Z, E_i)$  is the Fermi function.  $Z$  is the daughter nuclear charge;  $p$ ,  $E$  and  $E_i$  are the momentum, kinetic and total energy of  $\beta$  rays, respectively;  $\epsilon(E)$  is the correction for the accepting solid angle due to scanning potential[16];  $R(E, E_i)$  is the total resolution function;  $\alpha$  is the empirical shape correction factor used by Ref. [10];  $W_j$  and  $E_j$  are the branching ratio and excitation energy of the final state, taken from Ref. [20-22];  $m_\nu^2$  refers to (neutrino mass)<sup>2</sup>;  $BG$  represents the background;  $A$ ,  $E_0$ ,  $\alpha$ ,  $m_\nu^2$  and  $BG$  were free parameters in the fitting program[23].

Table 1 shows the effects of different final state structures(FSS). From this table, the differences among tritium containing molecules and tritium molecules in FSS effect are not remarkable; the  $m_\nu^2$  values deduced from T-atom and T-nuclei deviate much from zero. The measuring data for runs added into seven series and the fitting results of FSS of  $\text{CH}_3\text{T}$ [20] are shown in Table 2.

Fig. 5 shows the Kurie plots of the series 1-5, where the solid lines are the corresponding best fit for the data points. Fig. 6-a is the deviation of the best fit from data and the Fig. 6-b is that of the fit with  $m_\nu^2=900$  (eV<sup>2</sup>), divided by the standard deviation. It is seen that  $m_\nu^2=900$  (eV<sup>2</sup>) gives a poor fit.

Systematic errors were investigated by varying the input parameters. These are the different resolution functions of  $R_{th}$  and  $R_{exp}$ , the effective average source thickness and the final states parameters  $W_i, E_j$ .

1. The effect of different resolution functions of  $R_{th}$  and  $R_{exp}$  is to shift the resulting

$m_\nu^2$  by an amount of 27 (eV<sup>2</sup>).

2. The error of the effective average source thickness is 16%. This results in an effect of 29 (eV<sup>2</sup>) on  $m_\nu^2$ .
3. The uncertainties from the final state parameters  $W_0$  and  $E_j$  were taken to be the maximum variation in the results for CH<sub>3</sub>T [20]. That of  $W_0$  and  $E_j$  are 2% and 6%, respectively. The effect of varying each input parameter separately is to shift the fitted  $m_\nu^2$  by an amount of 11 (eV<sup>2</sup>) and 24 (eV<sup>2</sup>), respectively.

All of the above mentioned shifts of  $m_\nu^2$  were added in quadrature to yield systematic error as  $m_\nu^2(\text{syst.}) = \pm 48$  (eV<sup>2</sup>). The seven series of data sets are combined by taking a weighted average to obtain

$$m_\nu^2 = -31 \pm 75 \pm 48 \text{ (eV}^2\text{)}$$

The statistical and systematic errors added in quadrature and for  $m_\nu^2$  at 95% confidence level arrive at the final result as the upper limit on  $m_\nu^2$

$$m_\nu^2 < 155 \text{ (eV}^2\text{) or } m_\nu < 12.4 \text{ (eV), } E_0 = 18578.3 \pm 5.1 \text{ (eV).}$$

where an error of 5.1 eV was obtained by linearly adding with the statistical error (0.4 eV) and the systematic errors of the source alignment (1.4 eV) and the energy uncertainty of <sup>169</sup>Yb-M<sub>1</sub> line.

## 5 CONCLUSION

As mentioned above, the fitting results are sensitive to the FSS of the  $\beta$  source. So

the results of T-atom and T-nuclei are different from the FSS of our tritium-containing molecule source. But all the fitting based on the FSS have some systematic negative  $m_\nu^2$  values, which will be discussed in our next paper[25]. Some of the recent results of neutrino mass measurement are listed in Table 3. As can be seen, the last five results do not indicate any serious discrepancy among them, and all of them are disagreed with the finite neutrino mass of  $17 < m_\nu < 40$  eV reported by the ITEP group[2]. Up to now, whether the neutrino mass equals zero or not is still an open problem.

We would like to thank Professors Wang Gauchang and Dai Chuanzeng for their suggestions and supports on work and Professor Ho Tsohsiu for his theoretical consultation and helpful advices during this experiment. We are grateful to Jiang Weisheng, Li Yaohua, Chen Wenkui, the multichannel electronics group and the radiation protection group of CIAE for their excellent cooperation and helps during this experiment.

## REFERENCES

- [ 1 ] V.A. Lubimov, E.G. Novikov, V.Z. Nozik et al., *Phys. Lett.*, B 94 (1980) 266.
- [ 2 ] S. Boris, A. Golutvin, L. Laptin et al., *Phys. Rev. Lett.*, 58 (1987) 2019.
- [ 3 ] M. Fritschi, E. Holzschuh, W. Kundig et al., *Phys. Lett.*, B 137 (1986) 485.
- [ 4 ] H. Kawakami, S. Kato, T. Ohshima et al., *Phys. Lett.*, B 256 (1991) 105.
- [ 5 ] R.G.H. Robertson, T.J. Bowles, G.J. Stephenson et al., *Phys. Rev. Lett.*, 67 (1991) 957.
- [ 6 ] H. Daniel, K.H. Hiddemann, O. Schwentker et al., *Neutrino Mass and Related Topics*, Edited by S. Kato, T. Ohshima, (World Scientific, 1988), 125.

- [ 7 ] Mei Zhenyue, Ke Zunjian, Wu Weimin, et al., *Chinese Phys. Lett.*, 7 (1990) 345.
- [ 8 ] Sun Hancheng, Liang Dongqi, Chen Shiping et al., *Proc. Symp. on Nuclear Beta Decay and Neutrino*, (Osaka, 1986, world scientific), 322
- [ 9 ] Sun Hancheng, Liang Dongqi, Mao Naifeng et al., *IEEE, Tran. on Magnetics*, March, 24 (1988) 1346.
- [ 10 ] K.E. Bergkvist, *Nucl. Phys.*, B 39. (1972) 317.
- [ 11 ] Mao Naifeng, Liang Dongqi and Sun Hancheng, *Chinese Jour. of Nucl. Phys.*, 12. 2 (1990) 173
- [ 12 ] Liang Dongqi, Si Guojian, Lu Miaogen et al., *Ann. Report of CIAE*, (1982) 38 (in chinese).
- [ 13 ] Hu Nuanwen, Liang Dongqi, Wei Luncun et al., *Ann. Report of CIAE*, (1991)(in chinese).
- [ 14 ] Du Hongshan, Liang Dongqi, Wang Yusheng et al., *Chinese Journal of Atomic Energy Science and Technology*, 24. No. 4 (1990) 37 (in chinese).
- [ 15 ] Liang Shengzhu, Liang Dongqi and Xie Jun, *Nucl. Instr. and Meth.*, 5.(1985) 91 (in chinese).
- [ 16 ] Hu Zhonglin, "Neutrino Mass Measurement Using Organic  $^3\text{H}$  Source", M. S. Thesis, CIAE, 1985.
- [ 17 ] Liang Dongqi, Mao Yajun, Chen Shiping et al., *Ann. Report of CIAE*, (1991)

- [ 18 ] Xu Shuyan and Chen Shiping, *Chinese Journal of Computational Physics*, 3. 2 (1991) 183 (in chinese).
- [ 19 ] S. Boris, A. Golutvin, L. Laptin et al., *Phys. Lett.*, B 159 (1985) 217.
- [ 20 ] I.G. Kaplan, G.V. Smelov and V.N. Smutny, *Phys. Lett.*, B 161 (1985) 389.
- [ 21 ] Ching Chengrui and Ho Tsohsiu, *Phys. Reports*, 112, No. 1 (1984) 1.
- [ 22 ] R.L. Martin and J.S. Cohen, *Phys. Lett.*, B 110 (1985) 95.
- [ 23 ] Mao Yajun, Liang Dongqi, Chen Zhicai et al., *Ann. Report of CIAE*, (1991) (in chinese).
- [ 24 ] E. Holzschuh, M. Fritschi, W. Kundig, *Phys. Lett.*, B 237 (1992) 381.
- [ 25 ] Ching Chengrui, Ho Tsohsiu, Liang Dongqi, et al., (to be published).

Table 1. Results of the final state structures of  $\beta$  spectrum

FSS	No. of Levels	$W_0$	$E_t[21]$ (eV)	$\chi^2/DOF$	$E_0 - 18500$ (eV)	$m_\nu^2$ (eV) <sup>2</sup>
CH <sub>3</sub> T	2	0.6056	48.80	1.141	78.6	-71
CH <sub>3</sub> T[20]	7	0.6056		1.141	78.3	-31
CH <sub>2</sub> =CHT	2	0.6006	47.48	1.145	79.7	-51
CH <sub>3</sub> -CHT-CH <sub>3</sub>	2	0.6030	48.46	1.144	79.9	-43
VALINE II	2	0.6291	50.90	1.140	78.9	-141
T molecule	2	0.5820	44.98	1.148	79.9	-68
T molecule[22]	12	0.5822		1.145	77.6	-177
T atom	2	0.7020	45.65	1.146	75.2	-191
T nuclei	1	1.000		1.158	67.2	-237

Table 2. Summary of the fitting results

series	$\chi^2/DOF$	$E_0-18500$ (eV)	$\alpha (\times 10^{-3})$ (eV <sup>-2</sup> )	$m_\nu^2$ (eV <sup>2</sup> )
1	73/61	77.2 ± 1.1	0.85 ± 0.40	-89 ± 169
2	74/58	78.7 ± 1.1	0.78 ± 0.84	-287 ± 282
3	61/61	79.4 ± 1.3	-2.43 ± 0.92	364 ± 165
4	77/53	75.9 ± 1.1	-1.12 ± 0.47	-100 ± 154
5	67/59	79.8 ± 1.2	-1.64 ± 0.49	-109 ± 239
6	73/64	77.2 ± 1.2	0.98 ± 0.46	-14 ± 237
7	81/64	80.8 ± 1.2	-3.52 ± 0.52	-369 ± 262

Table 3. Electron anti-neutrino mass

Reference	$m_\nu^2$ (eV <sup>2</sup> )	$m_\nu^2$ Errors (eV <sup>2</sup> )		Quoted upper 95% $m_\nu$ limit (eV)
		Statistical	Systematic	
HEP[2] 1987	919	60	150	17 < $m_\nu$ < 40
Zurich[3] 1986	-11	63	178	18
INS[4] 1991	-65	85	65	13
LANL[5] 1991	-147	68	41	9.3
Zurich[24] 1992	-21	48	61	11
GAE 1992	-31	75	48	12.4

Figure captions

Fig. 1. The construction of the spectrometer and electron beam layout, where S- $\beta$  source, D-detector.

Fig. 2. Internal conversion lines of <sup>169</sup>Yb-M obtained at proper compensation potential.

Fig. 3. The total resolution.

Fig. 4. Pulse height spectra for <sup>3</sup>H- $\beta$  and <sup>55</sup>Fe-X.

Fig. 5. The Kurie plot for series 1-5.

Fig. 6. The deviation of a - the best fit and b - the fit with  $m_\nu^2 = 900$  (eV<sup>2</sup>), divided by the standard deviation.



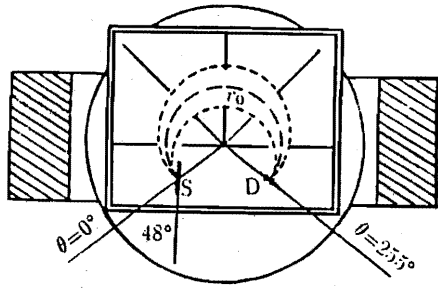


Fig.1 The construction of the spectrometer and electron beam layout. S-source, D-detector.

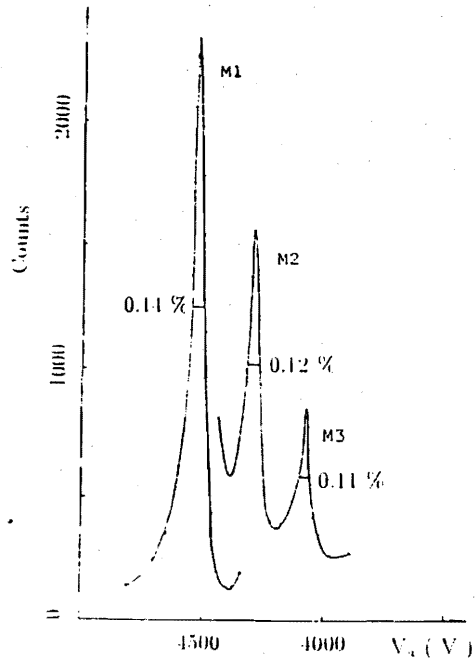


Fig.2 Internal conversion lines of  $^{169}\text{Yb-M}$  obtained at proper compensation potential.

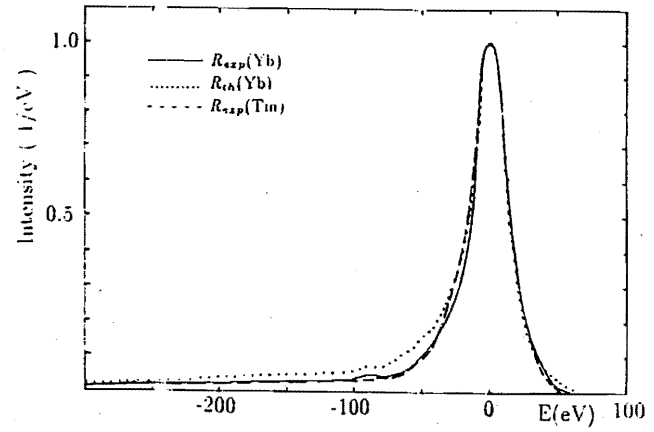


Fig.3 The total resolution function

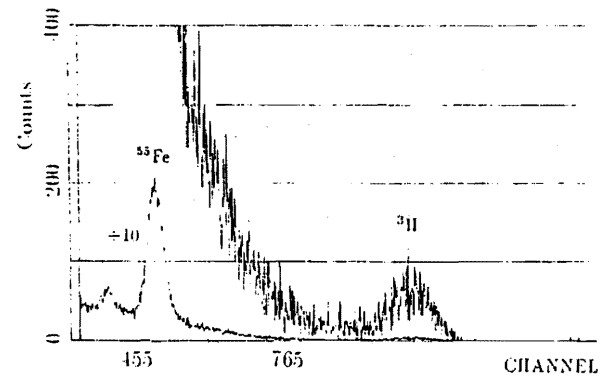


Fig.4 Pulse height spectra for  $^{311}\text{-B}$  and  $^{55}\text{Fe-X}$ .

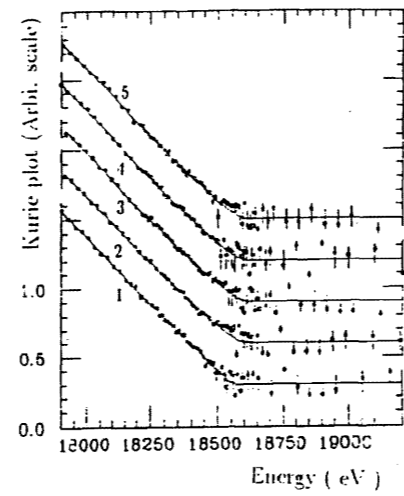


Fig.5 The Kurie plot for series 1-5

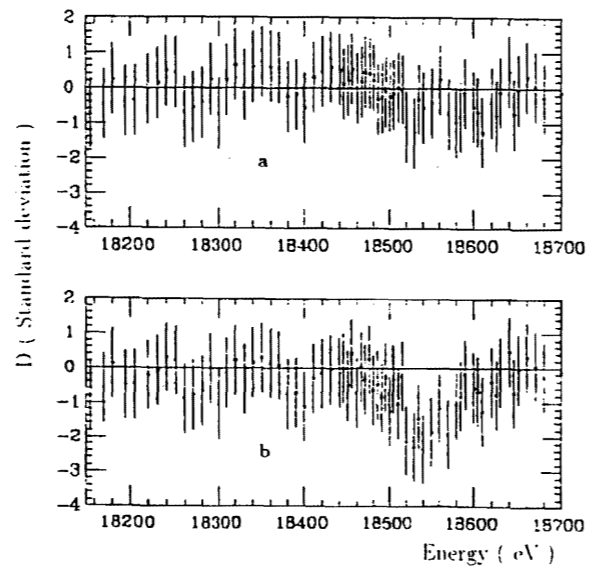


Fig.6 The deviation of a- the best fit and b- the fit with  $m_e^2=900 \text{ (eV}^2\text{)}$ , divided by the standard deviation.